Involvement of the JNK/HO-1/FTH1 signaling pathway in nanoplastic-induced inflammation and ferroptosis of BV2 microglia cells

JIAYIN SUN[1], YIHUA WANG[2], YILUN DU[3], WANXIN ZHANG[1], ZUODONG LIU[1], JIN BAI[1], GUANQUN CUI[4] and ZHONGJUN DU[1]

[1]Department of Toxicology, Shandong Academy of Occupational Health and Occupational Medicine, Shandong First Medical University and Shandong Academy of Medical Sciences, Jinan, Shandong 250062; [2]Department of Applied Chemistry, Chemical Institute of Chemical Industry, Xinjiang University of Science and Technology, Korla, Xinjiang 841000; [3]Articular Surgery, Affiliated Hospital of Qinghai University, Xining, Qinghai 810000; [4]Department of Respiratory Medicine, Children's Hospital Affiliated to Shandong University, Jinan, Shandong 250022, P.R. China

Received February 12, 2023; Accepted May 3, 2023

DOI: 10.3892/ijmm.2023.5264

Abstract. Nanoplastics (NPs) are a newly discovered type of environmental pollutant. The potential for neurotoxicity caused by NPs and their mechanisms are unclear. The present study aimed to determine the molecular mechanism underlying neurotoxicity induced by NPs. Microglia (BV2) cells were used for *in vitro* studies, and it was found that NPs invaded cells, activated inflammasomes, induced the release of significant quantities of inflammatory factors by detection of inflammatory response-associated proteins through Western blot and ELISA. By detection of FITC, SOD, GSH, cellular iron level, and ferroptosis-related proteins, it was found that NPs compromised the anti-oxidative mechanisms of cells, increased intracellular lipid peroxidation and Fe^{2+} concentration and triggered inflammatory reactions and ferroptosis. Pretreatment with reactive oxygen species (ROS) inhibitor N-acetylcysteine (NAC) alleviated induction of inflammatory reactions and ferroptosis of cells. In addition, inhibiting expression of c-Jun N-terminal kinase (JNK) increased expression of heme oxygenase (HO-1), resulting in decreased ferroptosis, indicating that the JNK/HO-1 signaling pathway was involved in NP-induced effects on ferroptosis in BV2 cells. In conclusion, NPs could induce inflammatory responses and ferroptosis in BV2 cells. JNK/HO-1 mediated ferroptosis may serve an important role in the toxicity of microglia induced by NPs. This study provided novel evidence for the toxic effects of NPs and highlighted a theoretical mechanistic basis for safe prevention and treatment of plastic pollution-induced neurotoxicity.

Correspondence to: Professor Zhongjun Du, Department of Toxicology, Shandong Academy of Occupational Health and Occupational Medicine, Shandong First Medical University and Shandong Academy of Medical Sciences, 18877 Jingshi Road, Lixia, Jinan, Shandong 250062, P.R. China
E-mail: duzj1981@163.com

Dr Guanqun Cui, Department of Respiratory Medicine, Children's Hospital Affiliated to Shandong University, 23976 Jingshi Road, Huaiyin, Jinan, Shandong 250022, P.R. China
E-mail: cuiguanqun1000@163.com

Abbreviations: NP, nanoplastic; ASC, apoptosis-associated speck-like protein; GSH, glutathione; MDA, malondialdehyde; SOD, superoxide dismutase; GPX4, glutathione peroxidase 4; HO-1, heme oxygenase; JNK, c-Jun N-terminal kinase; FTH1, ferritin heavy chain 1; TFRC, transferrin receptor; COX-2, cyclooxygenase-2; XCT, solute carrier family 7 member 11; NAC, N-acetylcysteine

Key words: nanoplastic, microglia, ferroptosis, inflammation, mechanism

Introduction

Plastic products are a newly discovered type of environmental pollutant. They are lightweight, waterproof, and can be reused. The technology for producing plastics is mature and the cost is very low. Their use is ubiquitous around the world, with an increasing trend. However, they do not degrade well under normal environmental conditions and thus serve as pollutants in numerous ecological environments (1,2). Only 21-26% of plastic waste is properly recycled and incinerated. The remaining plastic waste is incinerated in open air or discarded into the environment, leading to water, air, and soil being polluted by plastic waste (1-3). Reactions between plastic waste and environmental particulates/matter result in breakdown of plastic into smaller pieces of plastic, termed microplastics (MPs) (4-6). Nanoplastics (NPs) with a diameter of 1-100 nm are formed by degradation of MPs (diameter, 5 mm) (7) by weathering, solar radiation and biodegradation (8). MPs have been reported in foods such as mussels (9), commercial fish (10), sugar (11) and bottled water (12); thus the primary means of entry of MPs into the human body is likely ingestion.

MPs/NPs reach organs and tissues in the body after exposure. The liver is one of the first organs to encounter environmentally harmful substances (such as heavy metals, biotoxins, chemical residues or particulate matter) absorbed through the intestine and is subjected to multiple biochemical stresses such as inflammation and virus (13). The liver also harbors the most abundant macrophage pool, consisting of resident (Kupffer cells) and infiltrating bone marrow-derived macrophages (14). Macrophages are the second largest proportion of cells in the liver and they play key roles in the development of liver injury (15). Recent research has shown that MPs cause macrophage recruitment in the liver, and the macrophage infiltration rate in livers exposed to 1-10 μm MPs is greater than the large-diameter MPs, these data suggest that macrophage-driven mechanisms of action potentially play a key role in PS-MP-induced liver fibrosis (16). Zebrafish exposed to high concentrations of NPs exhibit notable changes in locomotor activity, aggression, school formation and predatory avoidance behaviors, as well as circadian dyskinesia following prolonged exposure. These changes highlight the potential neurotoxic effects of NP exposure (17). Expression of neuronal activity-dependent genes (cFos and Egr1) and synaptic proteins such as activity-regulated cytoskeleton-associated protein/activity-regulated gene 3.1, in mice exposed to MPs is altered, and neuroinflammation in the hippocampus is increased, followed by behavioral changes via a vagus-dependent pathway (18). The aforementioned studies indicated that the nervous system is a potential target organ for MP exposure. MPs pass through the blood-brain barrier (BBB), activate microglia and alter neurotransmitter release; however, the mechanism of microglial cytotoxicity caused by MPs requires further study.

Inflammation is a defensive response to remove infections and other toxic irritants, but inflammation can also cause significant damage and is hypothesized to be the cause of numerous types of disease such as atherosclerosis (19). Intracellular innate immune receptor NLRP3, adapter apoptosis-associated speck-like protein (ASC) and protease caspase-1 form a multi-protein complex called the NLRP3 inflammasome, which identifies pathogen- and damage-associated molecular patterns and collects and activates the inflammatory protease caspase-1 (20). Following long-term exposure to MPs/NPs, intracellular reactive oxygen species (ROS) production by mitochondria is increased, oxidative stress reactions occur and the NLRP3/caspase-1 signal pathway is activated, resulting in granulosa cell apoptosis and ovarian reserve reduction (21,22).

ROS serve as intracellular signaling molecules, mediating inflammation, apoptosis and pyroptosis in multiple types of cell (23). Excess iron promotes subsequent lipid peroxidation through the production of ROS via the iron-dependent Fenton reaction. The molecular mechanism of ferroptosis involves regulating the balance between oxidative damage and antioxidant defense (24). In addition, ROS are key signaling molecules that serve an important role in the progression of inflammatory disorders. Mitochondrial ROS signaling is a primary regulator of NLRP3 inflammasome activation (25). Thus, ROS serve key roles in the occurrence of ferroptosis and inflammatory reactions.

Ferroptosis is a special type of non-apoptotic regulatory cell death mechanism that is characterized by oxidative modification of phospholipid membranes via iron-dependent mechanisms, resulting in increased lipid peroxidation downstream of metabolic dysfunction (26,27). Biochemically, intracellular glutathione (GSH) is depleted, activity of GSH peroxidase 4 (GPX4) is reduced and the lipid peroxide cannot be metabolized by the reduction reaction catalyzed by GPX4. Fe^{2+} oxidizes lipids via the Fenton reaction, producing a large number of ROS and promoting ferroptosis (28,29).

JNK was discovered nearly 35 years ago and was originally discovered as a member of the pp54 microtubule-associated protein-2 kinase family (30,31). Combined exposure of alumina nanoparticles and chronic restraint stress compound hippocampal neuronal ferroptosis and activate the interferon-γ/apoptosis signal-regulating kinase 1/JNK signaling pathway, leading to learning and memory dysfunction in rats (32). It is not clear whether NPs, which are also nano particles, activate JNK and induce ferroptosis of microglia cells and the mechanism by which JNK is involved in ferroptosis remains unclear. Heme oxygenase (HO-1) is a key metabolic enzyme and is considered the central effector of mammalian stress responses (33,34). It has been hypothesized that HO-1 plays a regulatory role in apoptosis and autophagy, as well as in pyroptosis, necroptosis and ferroptosis (35). Notably, HO-1 is a key mediator of ferroptosis induced by erastin in cancer cells; Zinc protoporphyrin IX, an HO-1 inhibitor, prevents ferroptosis induced by erastin (36).

To understand the effects of NPs on human health and provide a basis for toxicological experiments, the present study investigated the molecular mechanisms of NP-induced microglial cell toxicity. An experimental *in vitro* model was established in which BV2 cells were exposed to NPs to induce an inflammatory reaction. N-acetylcysteine (NAC) was also used to evaluate the pivotal role of ROS in the inflammatory response and ferroptosis. Finally, we explored the toxicity and its mechanism of microglia induced by NP exposure.

Materials and methods

Characterization of polystyrene (PS-)NPs. Dragon Green-labeled NPs, which are the primary components of PS, were purchased from Bangs Laboratories, Inc. (cat. no. FSDG001). The mean diameter of PS-NPs was 44 nm and the solid content was 1%. The number of microspheres was ~$2.456x10^{14}$/ml deionized water. The size and shape of PS-NPs were detected by transmission electron microscopy (TEM; FEI Talos F200x). The sample was dispersed into an ethanol solution for ultrasound and then a few drops of the dispersed liquid were added onto a copper mesh. After drying, the sample was subjected to an accelerated voltage of 200 kV using FEI Talos F200X G2, EDS super-X, and the morphology was captured (high-resolution).

Cell culture and treatment. The mouse microglial cell line BV2 was obtained from Kunming Cell Bank of the Chinese Academy of Sciences (Kunming, China). BV2 cells were resuspended and cultured in DMEM (cat. no. C11995500BT) supplemented with 10% FBS (cat. no. 10099141; both Gibco; Thermo Fisher Scientific, Inc.) and 1% Antibiotic-Antimycotic (cat. no. 15240062; Gibco; Thermo Fisher Scientific, Inc.) and maintained in a humidified incubator supplied with 5% CO_2

at 37˚C. Cells were exposed to 0, 25, 50 or 100 μg/ml NPs for 12 h or 24 h at 37˚C. For inhibitor pretreatment groups, the ROS inhibitor NAC (10 μM; cat. no. S1623; Selleck) and JNK inhibitor SP600125 (2 μM; cat. no. S1460; Selleck) were added to cells for 2 and 1 h at 37˚C, respectively, and then BV2 cells were exposed to 50 μg/ml NPs for 12 h or 24 h at 37˚C. The nucleus of BV2 cells stained with DAPI (10 μg/ml; cat. no. C0065; Beijing Solarbio) for 5 h at room temperature.

Cell viability assay. Cell viability was determined using Cell Counting Kit-8 (CCK-8; cat. no. CK04; Dojindo Molecular Technologies, Inc.). NPs (10 mg/ml) were diluted to 0, 25, 50 and 100 μg/ml with serum-free DMEM and added to cells for 12 or 24 h at 37˚C. Subsequently, 10 μl CCK-8 solution was added for 2 h and the absorbance was measured at 450 nm using a microplate reader (SpectraMax 190; Molecular Devices, Inc.).

Determination of intracellular ROS concentration. BV2 cells were seeded with $3x10^5$ cells per well in six-well plates and exposed to NPs, as aforementioned, during the logarithmic growth phase. After 12 h at 37˚C, cells were incubated in DMEM containing 5 μM BODIPY™ 581/591 C11 probe for 30 min at 37˚C (cat. no. D3861, Thermo Fisher Scientific, Inc.) Cells were digested with Triple-E (Gibco; Thermo Fisher Scientific, Inc.) for 2 min at 37˚C. The cell precipitate was collected by centrifugation at 4˚C, 800 x g for 4 min and washed twice with PBS (Biological Industries; Sartorius AG). The cells were collected after being digested and blow down with a pipette, precipitated by centrifugation at 4˚C, 800 x g for 4 min and resuspended in 200 μl PBS. FITC in each group was measured using a flow cytometer (DxFLEX; Beckman Coulter, Inc.) with an excitation wavelength of 488 nm and emission wavelength of 510 nm. Annexin-V labeled with fluorescein FITC was used as a probe. And the software CytExpert for DxFLEX (version 2.0.0.283; Beckman Coulter, Inc.) used for analysis.

Determination of oxidative damage. BV2 cells in the logarithmic growth phase were used. Following exposure of cells to 50 μg/ml NPs for 12 h at 37˚C, cells were collected and the protein concentration was determined using a BCA protein assay kit. Malondialdehyde (MDA) levels (cat. no. S0131S; Beyotime Institute of Biotechnology) and activity of superoxide dismutase (SOD; cat. no. A001-3-2; Nanjing Jiancheng Bioengineering Institute) and GSH were detected using kits (cat. no. A006-2-1; Nanjing Jiancheng Bioengineering Institute) according to the manufacturer's protocols.

Inflammatory cytokine analysis. ELISA was performed to analyze inflammatory cytokines. Cell culture medium was collected and centrifuged for ~10 min (300 x g, 4˚C) and the supernatant was carefully collected. The levels of 1L-1β and IL-18 in supernatant of each sample were measured using corresponding mouse ELISA kits [cat. nos. EK201B/3-96 and EK218-96, respectively; both Hangzhou Lianke Biotechnology Co., Ltd.), according to the manufacturer's protocols.

Western blot analysis. RIPA lysis buffer (cat. no. P0013B) containing PMSF (cat. No. ST505; both Beyotime Institute of Biotechnology) was used to lyse BV2 cells treated with 0, 25, 50 and 100 μg/ml NPs for 12 h at 37˚C, on ice for 30 min and centrifuged at 15,000 x g for 15 min at 4˚C. The supernatant was obtained and the total protein concentration was determined using a BCA kit (Beyotime Institute of Biotechnology) and adjusted to the same quantity (44-46 μg) with PBS. The protein (44-46 μg/lane; 20 μl) was loaded on a 10% SDS gel, resolved using SDS-PAGE and transferred to PVDF membranes (MilliporeSigma). The membranes were blocked with blocking buffer (containing 5% milk powder) for 1 h at room temperature, washed three times with PBST (containing 0.1% Tween-20) and incubated with primary antibodies at 4˚C for 12 h. The following day, the membrane was incubated with fluorescent-labeled goat anti-rabbit or goat anti-mouse antibody for 1 h at 37˚C. Blots were visualized with Odyssey® CLx Imaging System (cat. no. 9140-00, LI-COR Biosciences). The gray values of the protein bands were analyzed using ImageLab™ Software (version no. 1.53 e). The primary antibodies were as follows: β-actin (1:1,000, cat. no. 4970S, Cell Signaling Technology, Inc.), NLRP3 (1:1,000, cat. no. ab263899, Abcam), cyclooxygenase (COX)-2 (1:1,000, cat. no. 12282, Cell Signaling Technology, Inc.), pro caspase-1 + p10 + p12 (1:1,000, cat. no. ab179515, Abcam), ferritin heavy chain 1 (FTH1) (1:1,000, cat. no. 3998, Cell Signaling Technology, Inc.), HO-1 (1:1,000, cat. no. 43966, Cell Signaling Technology, Inc.), ASC/Target of methylation-induced silencing (TMS1) (1:1,000, cat. no. 67824, Cell Signaling Technology, Inc.), GPX4 (1:1,000, cat. no. ab125066, Abcam), Acyl-CoA synthetase long-chain family member 4 (FACL4) (1:1,000, cat. no. ab155282; Abcam), Solute carrier family 7 member 11 (XCT) (1:1,000, cat. no. ab175186; Abcam), transferrin receptor (TFRC; 1:5,000, cat. no. ab269513, Abcam), JNK1 + JNK2 + JNK3 (1:1,000, cat. no. ab179461, Abcam) and JNK1 + JNK2 + JNK3 [phosphorylated (p)-T183 + T183 + T221; 1:5,000, cat. no. ab124956, Abcam]. The secondary antibodies were: IRDye® 680RD Goat anti-rabbit IgG (1:10,000, cat. no. 926-68071, LI-COR Biosciences) and IRDye® 800CW goat anti-mouse IgG (1:10,000, cat. no. 926-32210, LI-COR Biosciences). β-actin was used as an internal loading control for normalization.

Cellular iron level detection. BV2 cells were seeded in black 96-well plates at a density of $5x10^4$ cells/well and treated with NPs for 12 h, as aforementioned. The cells were incubated in 1X Hoechst (Beyotime Institute of Biotechnology) for 10 min at 37˚C, then with 1 μM FerroOrange (Dojindo Molecular Technologies, Inc.) for 30 min at 37˚C and the iron concentration in the cytoplasm was observed using a fluorescence microscope (x200).

Statistical analysis. Data were analyzed using GraphPad Prism version 9.0.0 (GraphPad Software, Inc.; Dotmatics, Inc.). Data were analyzed using ANOVA (one-way) followed by Dunnett's post hoc test. Data are presented as the mean ± SD of three independent repeats. $P<0.05$ was considered to indicate a statistically significant difference.

Results

Cytotoxicity of NPs to BV2 cells. The mean diameter of NPs was ~50 nm when single or multiple fluorescent microspheres

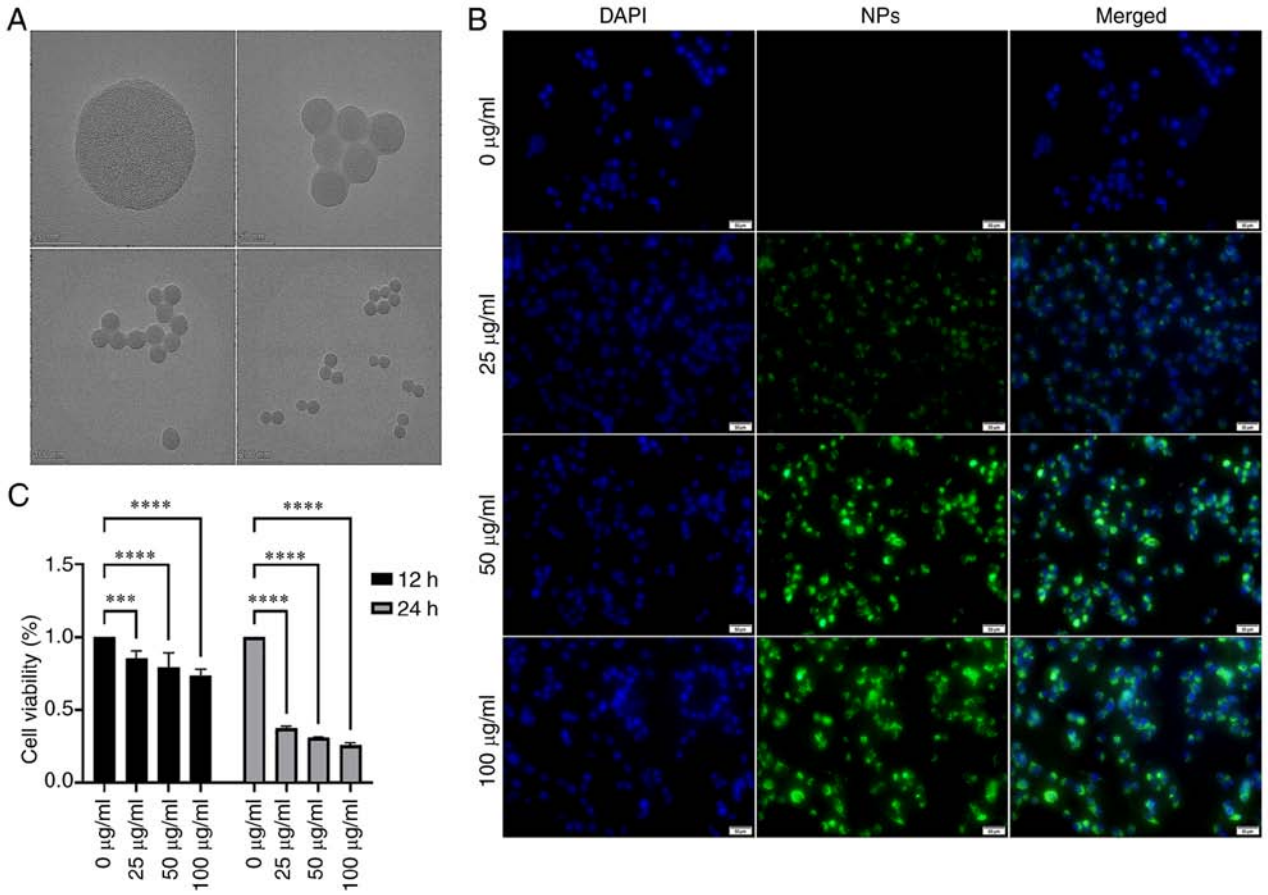

Figure 1. Cytotoxicity of NPs. (A) Characterization of NPs. (B) NPs enter BV2 cells. (C) Cell viability assay following treatment with NP for 12 or 24 h. NP, nanoplastic. ***P<0.001, ****P<0.0001.

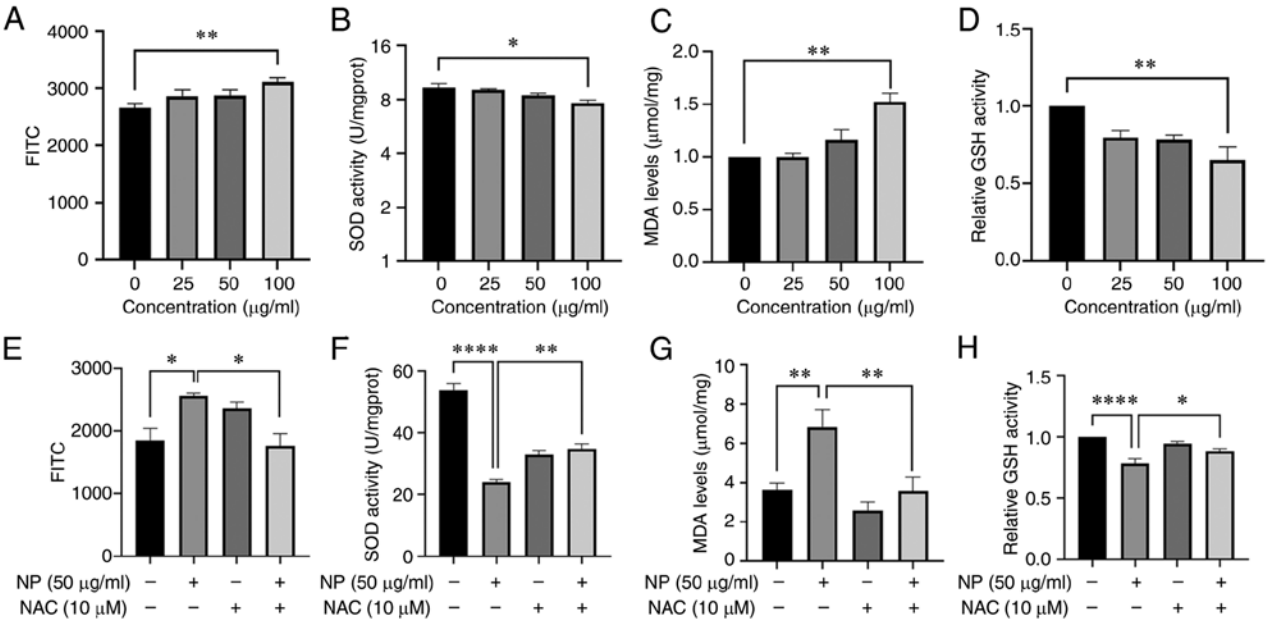

Figure 2. NP induces oxidative stress in BV2 cells. Following treatment with NPs, (A) FITC and (C) MDA levels increased in a dose-dependent manner, whereas (B) SOD and (D) GSH activity decreased. (E) FITC, (F) SOD, (G) MDA and (H) GSH in BV2 cells pretreated with 10 μM NAC followed by treatment with 50 μg/ml NP for 12 h. ROS, reactive oxygen species; MDA, malondialdehyde; SOD, superoxide dismutase; GSH, glutathione; NAC, N-acetylcysteine; NP, nanoplastic. *P<0.05, **P<0.01, ****P<0.0001.

were observed by TEM (Fig. 1A). BV2 cells exhibited green fluorescence following phagocytosis, and the intensity of fluorescence increased in a dose-dependent manner (Fig. 1B). This suggested that NPs were phagocytosed by microglia. The

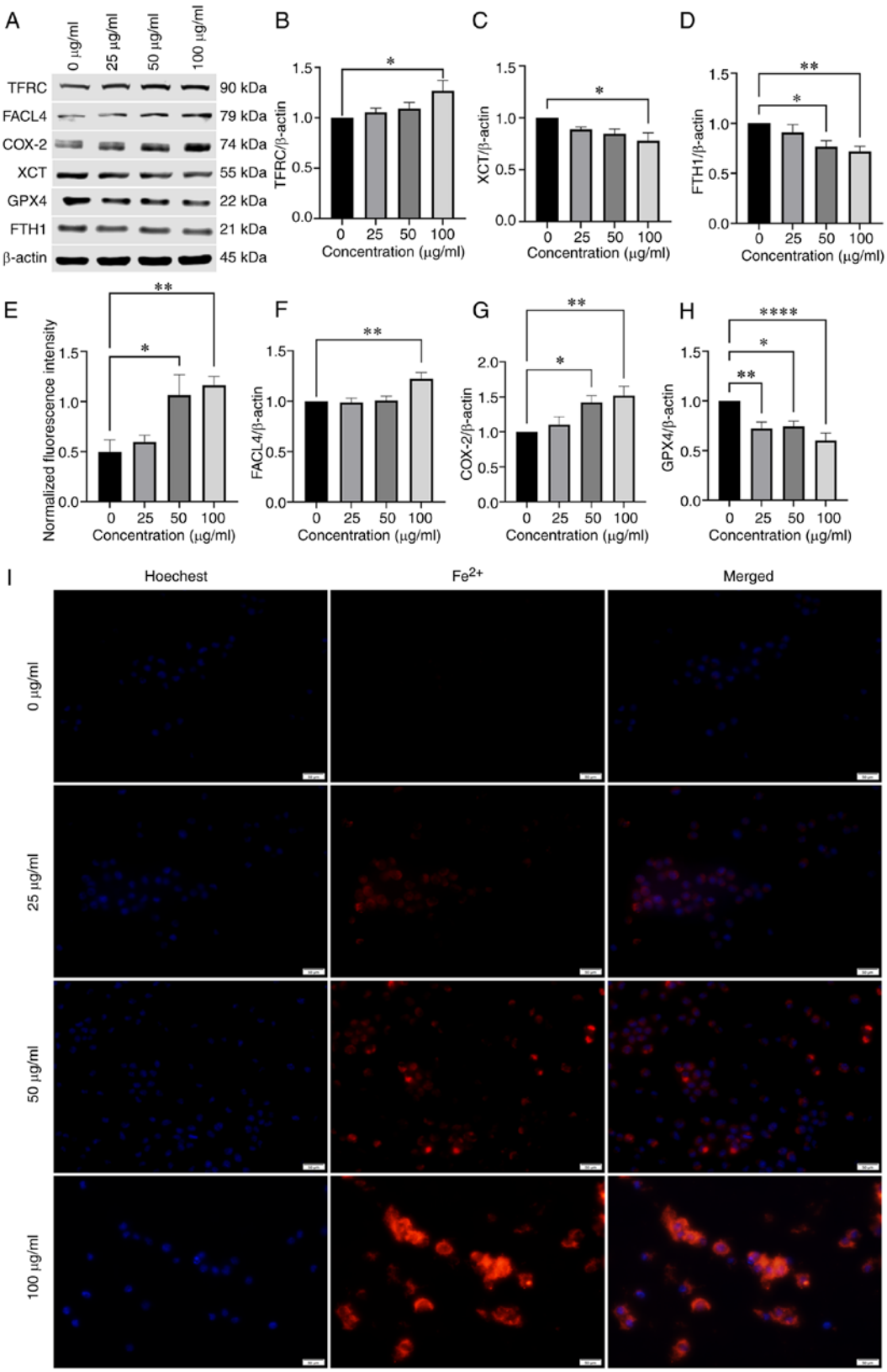

Figure 3. NP induces ferroptosis in BV2 cells. (A) Western blot analysis of ferroptosis-associated protein expression in BV2 cells treated with 0, 25, 50, or 100 μg/ml NPs for 12 h. (B) TFRC, (C) XCT, (D) FTH1, (E) Fluorescence intensity of Fe^{2+}, (F) FACL4, (G) COX-2, (H) GPX4, (I) Effect of NPs on Fe^{2+} content in BV2 cells using fluorescence microscope. NP, nanoplastic; TFRC, transferrin receptor; FACL4, acyl-CoA synthetase long-chain family member 4; COX-2, cyclooxygenase-2; XCT, solute carrier family 7 member 11; GPX4, glutathione peroxidase; FTH1, ferritin heavy chain 1. *P<0.05, **P<0.01, ****P<0.0001.

viability of BV2 cells after treated with NPs 12 h decreased obviously. The viability of BV2 cells exposed to 25, 50, 100 μg/ml NPs were lower than 0 μg/ml. After exposed to NPs 24 h, the viability of BV2 cells exposed to 25, 50, 100 μg/ml NPs substantially reduced and this effect was dose-and time-dependent (Fig. 1C).

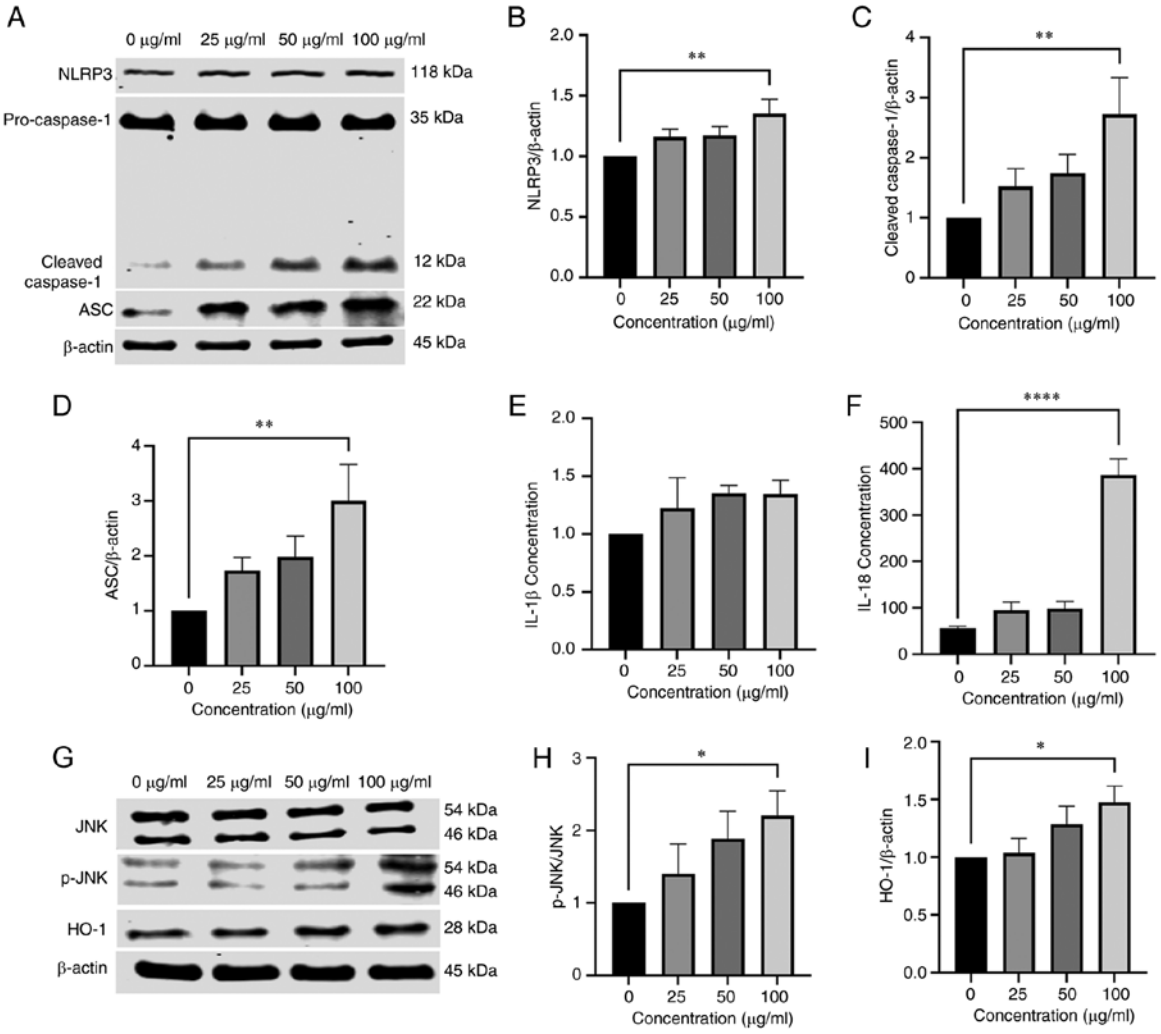

Figure 4. NPs cause inflammation and activate JNK and HO-1 in BV2 cells. (A) Detection of (B) NLRP3, (C) cleaved-caspase-1 and (D) ASC expression in BV2 cells by western blotting. Detection of IL-18 and (E) IL-1β and (F) IL-18 levels using ELISA. (G) Western blot analysis of the expression of (H) JNK, p-JNK and (I) HO-1 in BV2 cells treated with 0, 25, 50 or 100 μg/ml NP for 12 h. NP, nanoplastic; HO-1, heme oxygenase 1; ASC, apoptosis-associated speck-like protein; p-, phosphorylated. *P<0.05, **P<0.01, ****P<0.0001.

NPs induce oxidative damage in BV2 cells. To investigate whether NPs cause oxidative damage to BV2 cells, FITC following exposure to NPs for 12 h was measured. FITC in BV2 cells exposed to 100 μg/ml NPs increased significantly (Fig. 2A). MDA content increased 1.5x at 100 μg/ml compared with the untreated control group and was also notably higher than that of cells treated with lower concentrations of NPs (Fig. 2C). The activity of GSH (Fig. 2D) and SOD (Fig. 2B) decreased as the NP concentration increased. The activity of GSH and SOD decreased 1.6x and 1.2x, respectively, at 100 μg/ml NP compared with the control group. To confirm the impact of lipid oxidation on cell death, ROS inhibitor NAC was used. Compared with the 50 μg/ml NP group, the content of FITC (Fig. 2E) and MDA (Fig. 2G) in cells co-treated with NPs and NAC was significantly decreased. However, compared with the 50 μg/ml NP group, the activity of GSH (Fig. 2H) and SOD (Fig. 2F) in cells co-treated with NPs and NAC increased significantly.

NPs induce ferroptosis in BV2 cells. To verify whether NPs induced ferroptosis in BV2 cells, expression of ferroptosis-related proteins, including lipid peroxidation-associated indicators GPX4 and ACSL4 and XCT, was assessed. The protein levels of GPX4 and XCT in BV2 cells were downregulated by NPs (Fig. 3C and H) and protein expression of ACSL4 was upregulated (Fig. 3F). These results suggested that NPs stimulated lipid peroxidation in BV2 cells. The expression of TFRC and FTH1, which are responsible for ferritin transport (14), was also significantly altered; NPs downregulated the expression of FTH1 protein, while the levels of TFRC were increased (Fig. 3B and D). Using fluorescence microscopy, the mean fluorescence intensity of intracellular ions was shown to increase in a dose-dependent manner (Fig. 3E and I). Expression of COX-2 (Fig. 3G) also increased in a concentration-dependent manner.

NPs induce release of inflammatory factors and activate JNK, HO-1 in BV2 cells. The expression of inflammatory response-associated proteins in BV2 cells was determined using western blotting. The expression of NLRP3 and ASC in BV2 cells treated with 100 μg/ml NPs was significantly higher than in the control group (Fig. 4B and D). The ratio

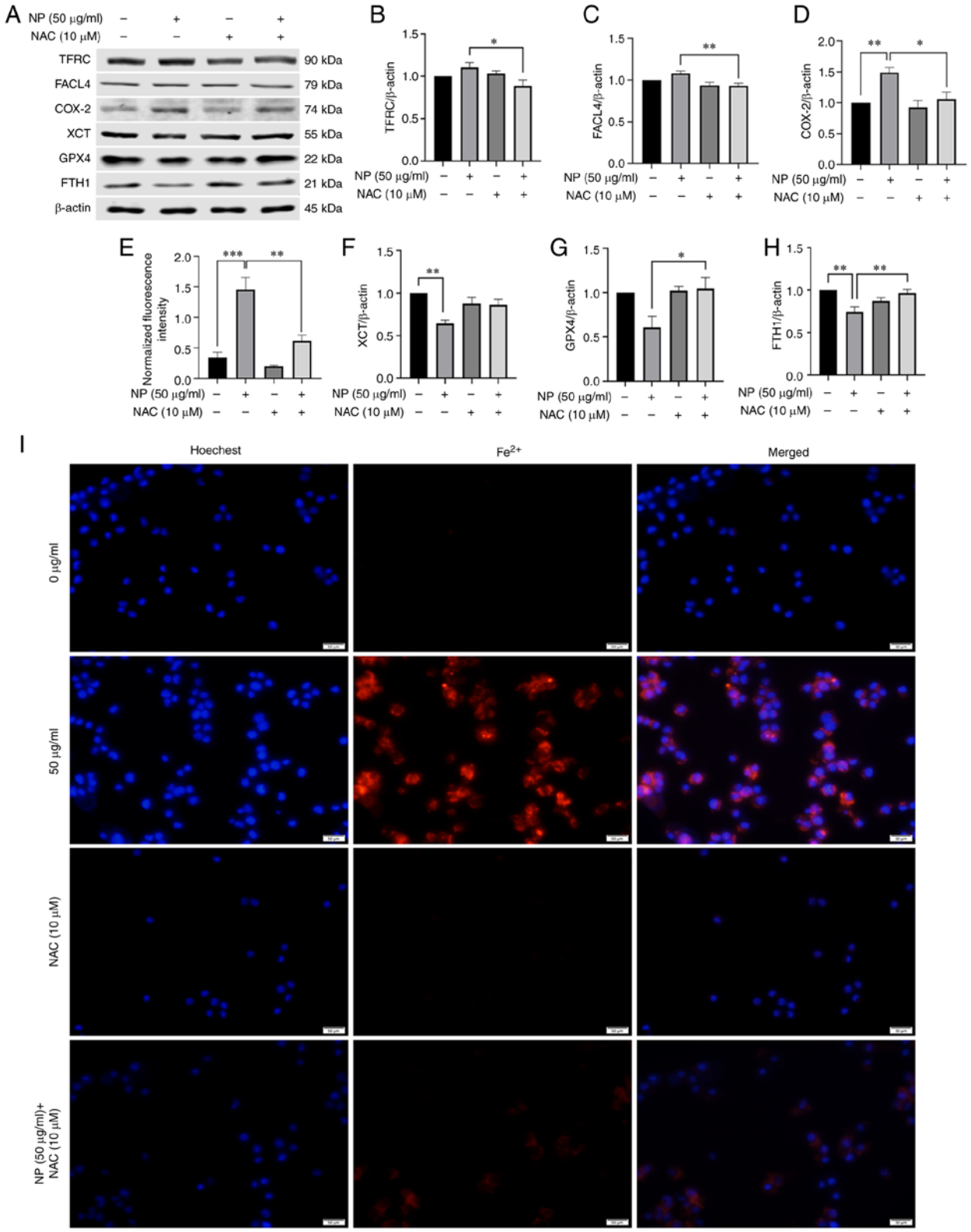

Figure 5. NAC inhibits NP-induced ferroptosis in BV2 cells. (A) BV2 cells were pretreated with SP600125 (2 μM) for 1 h and exposed to NPs for 12 h. The expression levels of ferroptosis-associated proteins were detected by western blotting. (B) TFRC, (C) FACL4, (D) COX-2, (E) Fluorescence intensity of Fe^{2+}, (F) XCT, (G) GPX4 and (H) FTH1 expression in BV2 cells pretreated with 10 μM NAC followed by treatment with 50 μg/ml NP for 12 h. (I) Mean fluorescence intensity of Fe^{2+} in BV2 cells determined using fluorescence microscopy. NP, nanoplastic; NAC, N-acetylcysteine; TFRC, transferrin receptor; FACL4, acyl-CoA synthetase long-chain family member 4; COX-2, cyclooxygenase-2; XCT, solute carrier family 7 member 11; GPX4, glutathione peroxidase; FTH1, ferritin heavy chain 1. *P<0.05, **P<0.01, ***P<0.001.

of cleaved-caspase-1 to pro-caspase-1 protein increased as the dose of NP increased, with 100 μg/ml NP increasing the ratio significantly compared with the control group (Fig. 4C). The expression levels of IL-1β increased evidently in cells treated with NPs compared with the control in a dose-dependent manner (Fig. 4E). To explore the impact of JNK and HO-1

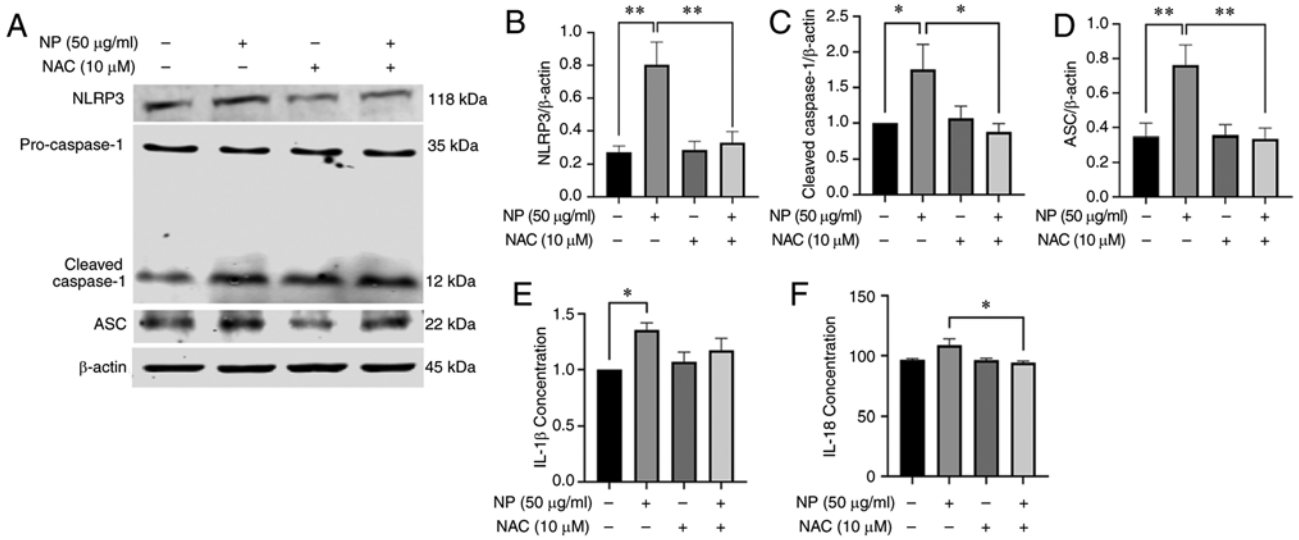

Figure 6. NAC inhibits NP-induced inflammation in BV2 cells. BV2 cells were pretreated with 10 μM NAC followed by treatment with 50 μg/ml NP for 12 h. (A) Expression of inflammation-associated protein was assessed using western blotting. (B) NLRP3, (C) cleaved caspase-1 and (D) ASC expression analysis. (E) IL-1β and (F) IL-18 in BV2 cells was assessed using ELISA. NP, nanoplastic; NAC, N-acetylcysteine; ASC, apoptosis-associated speck-like protein. *P<0.05, **P<0.01.

in NP-induced cytotoxicity, expression of p-JNK, JNK and HO-1 was detected using western blotting. Phosphorylation of JNK increased following treatment of NPs and the increase in p-JNK and HO-1 levels was dose-dependent (Fig. 4H and I). These results suggested that NPS induced activation of JNK and HO-1.

Increased ROS levels induce ferroptosis. ROS and lipid peroxidation induce cell death, such as by ferroptosis (14). NAC was used to determine whether ROS was involved in the regulation of ferroptosis. Cells were treated with 50 μg/ml NP and NAC to determine whether NPs induced ferroptosis was mediated by ROS. As aforementioned, NAC significantly decreased the expression of ROS, SOD, MDA and GSH and also decreased NP-induced oxidative damage. NAC inhibited the decrease in GPX4 expression (Fig. 5G). Compared with cells treated with NPs alone, the expression of FACL4 and TFRC decreased and the protein expression levels of XCT were increased following NAC pretreatment (Fig. 5B, C and F). Finally, compared with 0 μg/ml NPs group, the fluorescence intensity of the 50 μg/ml NPs group significantly grew larger. The fluorescence intensity in cells co-treated with NPs and NAC was significantly inhibited (Fig. 5E and I).

Inflammatory response is induced by NPs in a ROS-mediated-manner. To determine the effect of ROS on inflammatory reactions, NAC was used to inhibit ROS and levels of inflammatory cytokines, intracellular inflammation-associated proteins and inflammatory factors were assessed following NP treatment. Western blotting showed that NAC treatment resulted in downregulation of NLRP3, ASC and cleaved caspase-1 protein expression in BV2 cells (Fig. 6A-D). Following pretreatment with NAC, the expression of IL-18 and IL-1β also decreased significantly compared with cells treated with NPs alone (Fig. 6E and F). These results showed the key role of ROS in NP-induced inflammatory responses.

Ferroptosis is induced by the JNK/HO-1/FTH1 signaling pathway in a ROS mediated-manner. The aforementioned results indicated the important role of ROS in the inflammatory response and ferroptosis. NAC treatment inhibited JNK phosphorylation and downregulated HO-1 expression (Fig. 7B and C). To verify the role of JNK in ferroptosis, cells treated with NP were treated with JNK inhibitor SP600125. SP600125 inhibited downregulation of GPX4 and XCT (Fig. 7I and J), downregulated expression of TFRC and FACL4 protein (Fig. 7E and F) and upregulated the expression of the FTH1 protein (Fig. 7G). Compared with 0 μg/ml NP group, the fluorescence intensity of the 50 μg/ml NPs group significantly grew larger. The mean fluorescence intensity of intracellular iron ions was also significantly decreased following pretreatment of BV2 cells with SP600125 compared with 50 μg/ml NPs group (Fig. 7K and L).

Discussion

NPs are widely present in the environment, have disadvantageous effects on organisms and have received increasing attention (16-18,37). The number of NPs present in the environment is unknown as there are no effective methods to measure this. Due to the small size of NPs, they are extensively spread in aqueous environments and easily ingested by organisms (37). The aim of the present study was to investigate the possible effects of NPs on microglia.

Microglia are key cells of the immune system present in the central nervous system (38). Microglia comprise the innate immune system of the central nervous system and are key cellular mediators of neuroinflammatory processes. They serve a key role in central nervous system disease, including infection and acute and chronic neuroinflammatory responses (38). Chronic microglial activation is a key component of neurodegenerative disease and this chronic neuroinflammatory component likely contributes to neuronal dysfunction, injury and loss, leading to disease progression (38). BV2 cells are

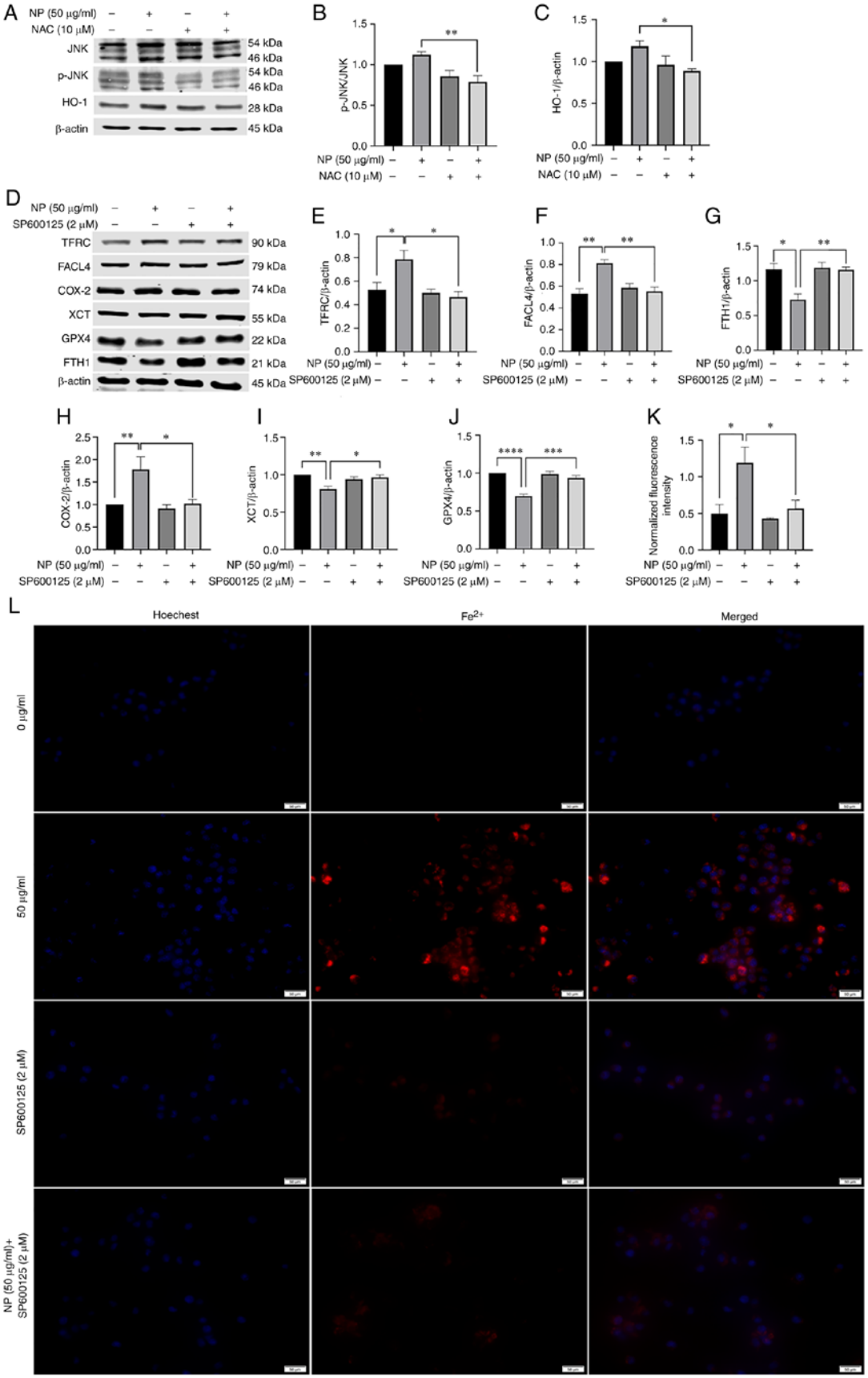

Figure 7. NPs regulate ROS to activate the JNK/HO-1/FTH1 signaling pathway to induce ferroptosis in BV2 cells. (A) NAC treatment downregulated expression of (B) JNK and (C) HO-1. (D) BV2 cells were pretreated with SP600125 (2 μM) for 1 h and exposed to NPs for 12 h. The expression levels of ferroptosis-associated proteins were detected by western blotting. NAC treatment downregulated expression of (E) TFRC, (F) FACL4 and (H) COX-2, upregulated expression of (G) FTH1, (I) XCT, (J) GPX4. (K) Fluorescence intensity of Fe^{2+}. (L) SP600125 treatment downregulated fluorescence intensity of Fe^{2+}. NP, nanoplastic; ROS, reactive oxygen species; HO-1, heme oxygenase 1; FTH1, ferritin heavy chain 1; p-, phosphorylated; TFRC, transferrin receptor; FACL4, acyl-CoA synthetase long-chain family member 4; COX-2, cyclooxygenase-2; XCT, solute carrier family 7 member 11; GPX4, glutathione peroxidase. *P<0.05, **P<0.01, ***P<0.001, ****P<0.0001.

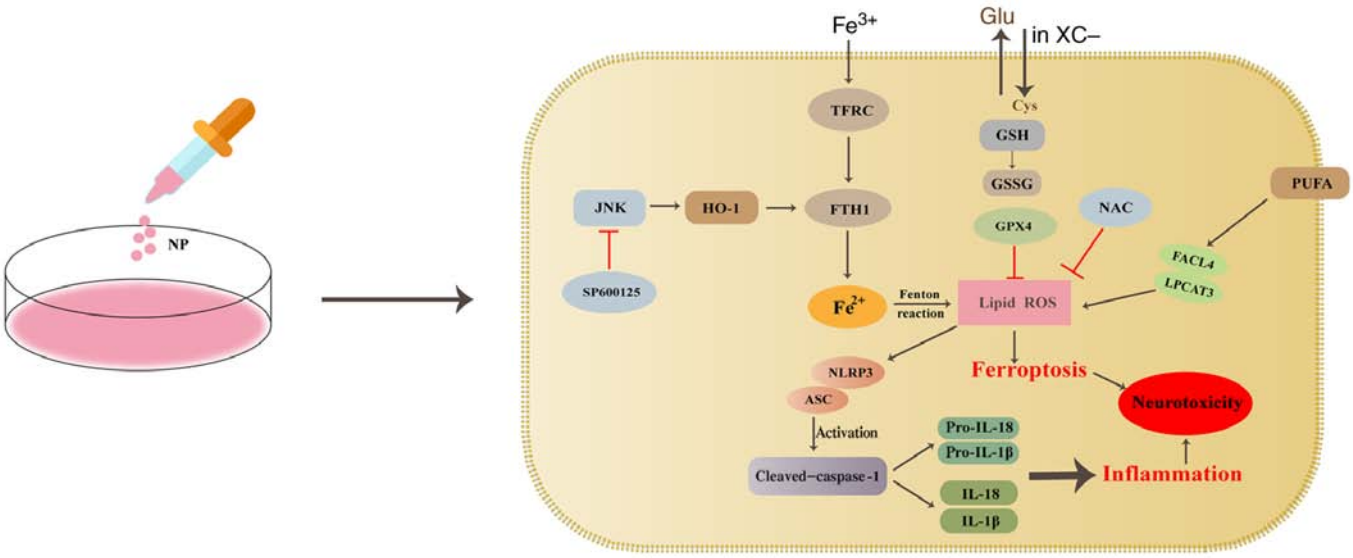

Figure 8. Schematic illustration of NP-induced inflammatory reactions and ferroptosis in BV2 cells. The primary function of system XC^- is to transport cystine and glutamate in and out of cells. Cysteine participates in GSH synthesis via system XC^-. GPX4 converts GSH to GSSG and inhibits ROS accumulation. Fe^{3+} binding to transferrin on the cell membrane is converted to Fe^{2+} and induces ferroptosis through lipid peroxidation via the Fenton reaction. NLRP3 is activated and interacts with ASC, resulting in cleavage of caspase-1 to mature cleaved caspase-1. Activated caspase-1 converts pro-IL-1β and pro-IL-18 to mature IL-1β and IL-18. GSH, glutathione; GPX4, glutathione peroxidase 4; ROS, reactive oxygen species; NP, nanoplastic; GSSG, glutathione disulfide; ASC, apoptosis-associated speck-like protein; HO-1, heme oxygenase 1; FTH1, ferritin heavy chain 1; TFRC, transferrin receptor; Glu, glutamate; Cys, cysteine; LPCAT3, lysophosphatidyltransferase 3; PUFA, polyunsaturated fatty acid.

immortalized cell lines of mouse microglia and were selected as the experimental model. Due to their small particle size, NPs can enter tissues and organs and cross the BBB. The breakdown of the BBB may result in an inflammatory response and neurodegeneration (40). Studies have shown that PS-NPs increase the permeability of the BBB, decrease dendritic spine density and induce an inflammatory response in the hippocampus and PS-NPs in microglia induce microglial activation and neuron damage in the mouse brain (39,40). The aforementioned results suggest that PS-NPs can pass through the BBB and induce neurotoxicity in mammals, potentially by inducing activation of microglia. Microglia, the resident macrophages of the central nervous system, rapidly activate in nearly all types of neurological disease. These activated microglia become highly motile, secrete inflammatory cytokines, migrate to the lesion area and phagocytose cell debris or damaged neurons. Even a minimal stimulus activates microglia and causes inflammation-induced neuronal damage (41). Kwon *et al* (42) found that PS-MPs in the brain co-localize with Ionized calcium binding adapter molecule 1, a marker of microglia, in all three regions (hippocampus, cortex, cerebellum). Shan *et al* (39) found that PS-NPs in microglia result in the activation of quiescent microglia, evidenced by transformation from a ramified to an amoeboid phenotype, enlargement of cell nuclei, stubby branches and reduced end-point voxels under Sholl analysis. The aforementioned results indicate that MPs can enter microglia and microglia can be activated. In the present study, the fluorescent signal of NPs in BV2 cells became stronger as the concentration of NPs increased.

ROS-mediated lipid peroxidation is key to ferroptosis. Cells have evolved a counterbalancing system to neutralize excess ROS, an antioxidant system consisting of enzymatic antioxidants such as SOD, catalase, GPX4 and thioredoxin (43). In the present study, when exposed to 100 μg/ml NPs, the levels of ROS increased significantly compared with the control group. The levels of GSH and SOD decreased, whereas MDA levels increased. From these results, it was speculated that NPs induced oxidative damage in BV2 cells.

Inflammation is a common immune response that leads to numerous types of dangerous and complex disease, such as atherosclerosis. Inflammasomes, which are multiprotein complexes, comprise Nod-like receptor (NLR), ASC and pro-caspase-1. Following assembly of inflammasomes, caspase-1 is activated and hydrolyzed into two products, forming a dimer to become mature cleaved caspase-1 (44). Activated caspase-1 cleaves pre-IL-1β and pre-IL-18 into mature IL-1β and IL-18. In the present study, expression of NLRP3, ASC and pro caspase-1 increased significantly following NP exposure and the expression of IL-18 and IL-1β also increased. ROS were shown to be the key mechanism triggering the formation and activation of the NLRP3 in the present study. Monocytes (MOs) serve as precursors of macrophage and effector cells, survey peripheral tissue and maintain endothelial integrity. Following inflammatory stimulus, MOs circulating in the bloodstream migrate to tissue and differentiate into either macrophages or MO-derived dendritic cells (MODCs) (45). MOs and MODCs release pro-inflammatory or anti-inflammatory cytokines that activate or suppress inflammation, respectively. In a recent study (46), PVC particles were shown to increase secretion of both pro-(IL-6 and TNF) and anti-inflammatory cytokines (IL-10) by MOs. The increase of both pro- and anti-inflammatory cytokine levels indicates the presence of a counterbalancing mechanism. NP exposure induces secretion of pro- and anti-inflammatory cytokines in primary human MOs and DCs (46).

Lysosome rupture is a mechanism of NLRP3 inflammasome activation. During lysosome rupture, cathepsin B is released from the lysosome. A previous study (19) showed that

cathepsin B binds to the leucine-rich repeat domain of NLRP3 and activates NLRP3. Cathepsin B is also involved in the activation of MAPKs, one of which is JNK. In addition, JNK inhibition decreases levels of IL-1β and activation of caspase-1; JNK1 and JNK2 participate in IL-1β cleavage (19). Ca^{2+} also activates JNK, a necessary kinase for ASC speck formation, by activating tat-associated kinase/JNK pathway (47). MAPKs control cellular activity, including gene expression, mitosis, differentiation, cell survival and apoptosis (48). In particular, MAPKs (ERK, p38 and JNK) have key roles in regulating inflammatory and immune responses (49). A previous study (50) indicated that ROS was upstream of MAPKs/NF-κB/NLRP3 and regulated expression of components involved in this pathway. Furthermore, to explore the sequence of MAPKs, nuclear NF-κB and NLRP3 in the inflammatory response induced by high glucose (HG), specific inhibitors of p38 (SB203580), ERK (PD98059) and JNK (SP600125) were used to pretreat osteoclasts (OCs) before induction with HG. SP600125, PD98059 and SB203580 significantly inhibited production of nuclear NF-κB, p-IκB, inhibitor of κB kinase and NLRP3 components (ASC, caspase-1, IL-18, IL-1β and NLRP3) and secretion of IL-1β and IL-18. These results showed that p-JNK, p-ERK1/2 and p-p38 mediated the activation of nuclear NF-κB-associated proteins and the NLRP3 inflammasome by HG in OCs. Together, these data demonstrated that the ROS/MAPK/NF-kB pathway regulates the HG-induced NLRP3 inflammasome response *in vitro* (50). Adiponectin suppresses palmitate-mediated NLRP3 inflammasome activation in hepatocytes via AMPK/JNK/ERK1/NF-κB/ROS signaling pathways (51). Past studies have shown that the JNK/c-Jun pathway serves crucial roles in the microglial response and kaempferol attenuates retinal ganglion cell death by suppressing the NLRP3 inflammasome through JNK pathways in acute glaucoma (52,53). A previous study (54) indicated that indirect traumatic optic neuropathy induces significant retinal ganglion cell (RGC) death and axonal degeneration and activates JNK/c-Jun signaling, which could further induce the microglial response and NLRP3 inflammasome activation. Moreover, JNK disruption suppresses NLRP3 inflammasome activation in microglia and prevents RGC death and axonal degeneration (54). A previous study found that spleen tyrosine kinase (Syk) and JNK are rapidly phosphorylated during *Staphylococcus aureus* infection. Moreover, a Syk/JNK inhibitor and Syk/JNK small interfering RNA not only decrease NLRP3 inflammasome-associated molecule expression at the protein and mRNA levels, ASC speck formation and IL-1β and IL-18 release but also rescue decreased NIMA-related kinase 7 (NEK7) expression following suppression of the NEK7/NLRP3 pathway in macrophages (55). Syk/JNK phosphorylation levels and NLRP3 inflammasome-associated molecule expression are decreased by blockade of K^+ efflux (55). The aforementioned studies indicate that NPs induce JNK to activate NLRP3 inflammatory vesicles and induce inflammatory response. The present study was not designed to prove the chronological association between activation of JNK and inflammatory response.

In the present study, NLRP3 was activated and protein expression levels of ASC, cleaved caspase-1, IL-18 and IL-1β increased significantly following exposure to NPs. NLRP3, ASC, cleaved caspase-1, IL-18, and IL-1β were all significantly downregulated by ROS inhibitor NAC. Thus, it was suggested that NPs induced microglia toxicity by increasing ROS levels, in turn inducing inflammatory responses.

System XC^- is an amino acid antiporter that is abundant in the phospholipid bilayer. It transports extracellular cystine and intracellular glutamate at a ratio of 1:1 and reduces cystine to cysteine in the cell. Inhibition of the activity of system XC^- decreases GSH synthesis by inhibiting cysteine uptake, leading to decreased GPX activity and decreased cellular antioxidant capacity, accumulation of lipid ROS and finally oxidative damage and ferroptosis (56). As a member of the GPX family, GPX4 primarily inhibits lipid peroxidation and serves an important role in the occurrence of ferroptosis. GSH serves as a cofactor in reduction of peroxide to the corresponding alcohol by GPX4. Thus, intracellular GSH is key for GPX4 activity (57,58). The results of the present study showed that exposure to NPs inhibited activity of system XC^-; levels of GSH were significantly decreased and activity of GPX4 was also inhibited. The aforementioned results demonstrated that NPs may cause lipid peroxidation, leading to ferroptosis.

Iron is a key trace element that participates in normal hematopoietic and immune function of the human body. Excessive iron cause lesions and damage to numerous types of tissue and organ. The key to the induction of ferroptosis is the accumulation of a large quantity of free iron in cells. Cells take up iron primarily via TF and TFRC 1, which are the primary iron uptake proteins. Excess iron must be removed via FTH1 and FTL, thereby avoiding the formation of ROS (14). The present study demonstrated that intracellular ferritin levels increased following NP exposure and the expression of TFRC protein increased in a dose-dependent manner. The expression of FTH1 decreased in a dose-dependent manner due to accumulation of excess ferritin in the cells. Lipid metabolism is a key factor in ferroptosis. Polyunsaturated fatty acids are susceptible to lipid peroxidation and are key elements of ferroptosis (15). Acyl CoA synthase long-chain family member 4 (ACSL4) and lysophosphatidyltransferase 3 (LPCAT3) activate polyunsaturated fatty acids. ACSL4 catalyzes free arachidonic acid (AA)/adrenic acid (AdA) binding to CoA to form AA/AdA-CoA derivatives. LPCAT3 catalyzes the biosynthesis of AA/AdA-CoA and membrane phosphatidylethanolamine (PE) to form AA/AdA-PE, which is an intermediate process to activate ferroptotic signals (59). Therefore, decreasing ACSL4 and LPCAT3 levels inhibits ferroptosis (60). In the present study, expression levels of FACL4 were significantly increased following exposure to NPs. Following pretreatment of BV2 cells with NAC, compared with the 50 μg/ml NP group, system XC^- and GSH activity were increased and the downregulation of GPX4 was reversed. Ferritin accumulation and transferrin expression decreased, FTH1 levels increased, lipid peroxidation was inhibited and FACL4 expression was downregulated. The aforementioned results demonstrated that lipid peroxidation and accumulation of ROS may be involved in multiple pathways associated with ferroptosis. NPs may induce lipid peroxidation and ROS accumulation, thus causing microglial ferroptosis. The primary function of system XC^- is to transport cystine and glutamate in and out of cells. Cysteine participates in GSH synthesis via system XC^-. GPX4 converts GSH to GSSG and inhibits ROS accumulation. Fe^{3+} binding to transferrin on the cell membrane is converted to Fe^{2+} and

induces ferroptosis through lipid peroxidation via the Fenton reaction. NLRP3 is activated and interacts with ASC, resulting in cleavage of caspase-1 to mature cleaved caspase-1. Activated caspase-1 converts pro-IL-1β and pro-IL-18 to mature IL-1β and IL-18 (Fig. 8).

JNK is activated by cytokines and environmental stressors such as ultraviolet irradiation and oxidative stress and belongs to a subset of MAP agonists (61). In the present study, NPs activated JNK. It was hypothesized that ROS generated following exposure to NPs activated the JNK pathway. To confirm this, cells were treated with ROS inhibitor NAC; expression of JNK in the NP + NAC group was notably lower than in the 50 μg/ml NPs group. Therefore, the increase in ROS was caused by activation of JNK. Previous studies have suggested that the regulation of HO-1 is mediated via MAPKs, including the ERK, JNK and p38 MAPK pathways (62,63). In the present study, following addition of the JNK inhibitor SP600125, the expression of HO-1 decreased, expression of FTH1 was increased and iron accumulation was decreased. Therefore, it was hypothesized that NPs induced ferroptosis in BV2 cells via the JNK/HO-1/FTH1 pathway.

There are limitations to this study. A limitation is that the present study was an *in vitro* study of NP-induced phenotype and mechanism. And the present study was not designed to prove that the phagocytosis of microglia occurred in a relatively short time. Future experiments should explore whether phagocytosis of pathogens and/or cell debris by microglia is affected by exposure to NPs.

The present study showed that NPs entered BV2 cells and induced oxidative stress and inflammatory responses. NPs also led to ferroptosis of BV2 cells via increased lipid peroxidation and ROS accumulation. ROS served a pro-ferroptotic role in NP-induced inflammatory responses and ferroptosis. NPs potentially induced ferroptosis by regulating the JNK/HO-1/FTH1 signaling pathway. The present study highlighted a novel avenue for the study of the pathogenesis and treatment of NP-induced central nervous system disease.

Acknowledgements

Not applicable.

Funding

The present study was supported by the National Natural Science Foundation of China (grant no. 81602893), the Natural Science Foundation of Shandong Province (grant nos. ZR2015YL049, ZR2021MH218 and ZR2022MH184), the Key Technology Research and Development Plan of Shandong Province (grant no. 2018GSF118018), Jinan Science and Technology Project (grant nos. 201907022 and 202019183) and the Innovation Project of Shandong Academy of Medical Science and Academic Promotion Programme of Shandong First Medical University (grant no. 2019QL001).

Availability of data and materials

The datasets used and/or analyzed during the current study are available from the corresponding author on reasonable request.

Authors' contributions

JYS, YHW, YLD, WXZ, GQC and ZJD conceived and designed the study. ZDL, GQC, JYS, YHW, YLD, WXZ and JB performed the experiments. JYS wrote the manuscript. GQC and ZJD provided funding and project administration, acquired and analyzed the data and critically reviewed and edited the manuscript. All authors have read and approved the final manuscript. All authors confirm the authenticity of all the raw data.

Ethics approval and consent to participate

Not applicable.

Patient consent for publication

Not applicable.

Competing interests

The authors declare that they have no competing interests.

References

1. Geyer R, Jambeck JR and Law KL: Production, use, and fate of all plastics ever made. Sci Adv 3: e1700782, 2017.
2. Rhodes CJ: Plastic pollution and potential solutions. Sci Prog 101: 207-260, 2018.
3. Liu J, Lezama N, Gasper J, Kawata J, Morley S, Helmer D and Ciminera P: Burn pit emissions exposure and respiratory and cardiovascular conditions among airborne hazards and open burn pit registry participants. J Occup Environ Med 58: e249-e255, 2016.
4. Kubowicz S and Booth AM: Biodegradability of plastics: Challenges and misconceptions. Environ Sci Technol 51: 12058-12060, 2017.
5. Avio CG, Gorbi S and Regoli F: Plastics and microplastics in the oceans: From emerging pollutants to emerged threat. Mar Environ Res 128: 2-11, 2017.
6. Waring RH, Harris RM and Mitchell SC: Plastic contamination of the food chain: A threat to human health? Maturitas 115: 64-68, 2018.
7. Jambeck JR, Geyer R, Wilcox C, Siegler TR, Perryman M, Andrady A, Narayan R and Law KL: Marine pollution. Plastic waste inputs from land into the ocean. Science 347: 768-771, 2015.
8. Thompson RC, Olsen Y, Mitchell RP, Davis A, Rowland SJ, John AW, McGonigle D and Russell AE: Lost at sea: Where is all the plastic? Science 304: 838, 2004.
9. Li J, Qu X, Su L, Zhang W, Yang D, Kolandhasamy P, Li D and Shi H: Microplastics in mussels along the coastal waters of China. Environ Pollut 214: 177-184, 2016.
10. Neves D, Sobral P, Ferreira JL and Pereira T: Ingestion of microplastics by commercial fish off the Portuguese coast. Mar Pollut Bull 101: 119-126, 2015.
11. Liebezeit G and Liebezeit E: Non-pollen particulates in honey and sugar. Food Addit Contam Part A Chem Anal Control Expo Risk Assess 30: 2136-2140, 2013.
12. Ossmann BE, Sarau G, Holtmannspotter H, Pischetsrieder M, Christiansen SH and Dicke W: Small-sized microplastics and pigmented particles in bottled mineral water. Water Res 141: 307-316, 2018.
13. Marra F and Tacke F: Roles for chemokines in liver disease. Gastroenterology 147: 577-594.e1, 2014.
14. MacKenzie EL, Iwasaki K and Tsuji Y: Intracellular iron transport and storage: From molecular mechanisms to health implications. Antioxid Redox Signal 10: 997-1030, 2008.
15. Yang WS and Stockwell BR: Ferroptosis: Death by lipid peroxidation. Trends Cell Biol 26: 165-176, 2016.

16. Wang S, Chen L, Shi X, Wang Y and Xu S: Polystyrene microplastics-induced macrophage extracellular traps contributes to liver fibrotic injury by activating ROS/TGF-β/Smad2/3 signaling axis. Environ Pollut 324: 121388, 2023.
17. Sarasamma S, Audira G, Siregar P, Malhotra N, Lai YH, Liang ST, Chen JR, Chen KH and Hsiao CD: Nanoplastics cause neurobehavioral impairments, reproductive and oxidative damages, and biomarker responses in zebrafish: Throwing up alarms of widespread health risk of exposure. Int J Mol Sci 21: 1410, 2020.
18. Lee CW, Hsu LF, Wu IL, Wang YL, Chen WC, Liu YJ, Yang LT, Tan CL, Luo YH, Wang CC, *et al*: Exposure to polystyrene microplastics impairs hippocampus-dependent learning and memory in mice. J Hazard Mater 430: 128431, 2022.
19. Hoseini Z, Sepahvand F, Rashidi B, Sahebkar A, Masoudifar A and Mirzaei H: NLRP3 inflammasome: Its regulation and involvement in atherosclerosis. J Cell Physiol 233: 2116-2132, 2018.
20. Kim YG, Kim SM, Kim KP, Lee SH and Moon JY: The role of inflammasome-dependent and inflammasome-independent NLRP3 in the kidney. Cells 8: 1389, 2019.
21. Hou J, Lei Z, Cui L, Hou Y, Yang L, An R, Wang Q, Li S, Zhang H and Zhang L: Polystyrene microplastics lead to pyroptosis and apoptosis of ovarian granulosa cells via NLRP3/Caspase-1 signaling pathway in rats. Ecotoxicol Environ Saf 212: 112012, 2021.
22. Wang F, Salvati A and Boya P: Lysosome-dependent cell death and deregulated autophagy induced by amine-modified polystyrene nanoparticles. Open Biol 8: 170271, 2018.
23. Latunde-Dada GO: Ferroptosis: Role of lipid peroxidation, iron and ferritinophagy. Biochim Biophys Acta Gen Subj 1861: 1893-1900, 2017.
24. Chen X, Kang R, Kroemer G and Tang D: Broadening horizons: The role of ferroptosis in cancer. Nat Rev Clin Oncol 18: 280-296, 2021.
25. Forrester SJ, Kikuchi DS, Hernandes MS, Xu Q and Griendling KK: Reactive oxygen species in metabolic and inflammatory signaling. Circ Res 122: 877-902, 2018.
26. Friedmann Angeli JP, Krysko DV and Conrad M: Ferroptosis at the crossroads of cancer-acquired drug resistance and immune evasion. Nat Rev Cancer 19: 405-414, 2019.
27. Conrad M and Pratt DA: The chemical basis of ferroptosis. Nat Chem Biol 15: 1137-1147, 2019.
28. Yang WS and Stockwell BR: Synthetic lethal screening identifies compounds activating iron-dependent, nonapoptotic cell death in oncogenic-RAS-harboring cancer cells. Chem Biol 15: 234-245, 2008.
29. Friedmann Angeli JP, Schneider M, Proneth B, Tyurina YY, Tyurin VA, Hammond VJ, Herbach N, Aichler M, Walch A, Eggenhofer E, *et al*: Inactivation of the ferroptosis regulator Gpx4 triggers acute renal failure in mice. Nat Cell Biol 16: 1180-1191, 2014.
30. Kyriakis JM and Avruch J: pp54 microtubule-associated protein 2 kinase. A novel serine/threonine protein kinase regulated by phosphorylation and stimulated by poly-L-lysine. J Biol Chem 265: 17355-17363, 1990.
31. Pulverer BJ, Kyriakis JM, Avruch J, Nikolakaki E and Woodgett JR: Phosphorylation of c-jun mediated by MAP kinases. Nature 353: 670-674, 1991.
32. Zhang H, Jiao W, Cui H, Sun Q and Fan H: Combined exposure of alumina nanoparticles and chronic stress exacerbates hippocampal neuronal ferroptosis via activating IFN-γ/ASK1/JNK signaling pathway in rats. J Hazard Mater 411: 125179, 2021.
33. Abraham NG and Kappas A: Pharmacological and clinical aspects of heme oxygenase. Pharmacol Rev 60: 79-127, 2008.
34. Ryter SW, Alam J and Choi AM: Heme oxygenase-1/carbon monoxide: From basic science to therapeutic applications. Physiol Rev 86: 583-650, 2006.
35. Ryter SW: Heme oxgenase-1, a cardinal modulator of regulated cell death and inflammation. Cells 10: 515, 2021.
36. Kwon MY, Park E, Lee SJ and Chung SW: Heme oxygenase-1 accelerates erastin-induced ferroptotic cell death. Oncotarget 6: 24393-24403, 2015.
37. Shen M, Zhang Y, Zhu Y, Song B, Zeng G, Hu D, Wen X and Ren X: Recent advances in toxicological research of nanoplastics in the environment: A review. Environ Pollut 252(Pt A): 511-521, 2019.
38. Streit WJ, Mrak RE and Griffin WS: Microglia and neuroinflammation: A pathological perspective. J Neuroinflammation 1: 14, 2004.
39. Shan S, Zhang Y, Zhao H, Zeng T and Zhao X: Polystyrene nanoplastics penetrate across the blood-brain barrier and induce activation of microglia in the brain of mice. Chemosphere 298: 134261, 2022.
40. Jin H, Yang C, Jiang C, Li L, Pan M, Li D, Han X and Ding J: Evaluation of neurotoxicity in BALB/c mice following chronic exposure to polystyrene microplastics. Environ Health Perspect 130: 107002, 2022.
41. Fu R, Shen Q, Xu P, Luo JJ and Tang Y: Phagocytosis of Microglia in the Central Nervous System Diseases. Mol Neurobiol 49: 1422-1434, 2014.
42. Kwon W, Kim D, Kim HY, Jeong SW, Lee SG, Kim HC, Lee YJ, Kwon MK, Hwang JS, Han JE, *et al*: Microglial phagocytosis of polystyrene microplastics results in immune alteration and apoptosis in vitro and in vivo. Sci Total Environ 807(Pt 2): 150817, 2022.
43. Nelson BA: A comprehensive program for pregnant adolescents: Parenting and prevention. Child Welfare 68: 57-60, 1989.
44. Sollberger G, Strittmatter GE, Garstkiewicz M, Sand J and Beer HD: Caspase-1: The inflammasome and beyond. Innate Immun 20: 115-125, 2014.
45. Teh YC, Ding JL, Ng LG and Chong SZ: Capturing the fantastic voyage of monocytes through time and space. Front Immunol 10: 834, 2019.
46. Weber A, Schwiebs A, Solhaug H, Stenvik J, Nilsen AM, Wagner M, Relja B and Radeke HH: Nanoplastics affect the inflammatory cytokine release by primary human monocytes and dendritic cells. Environ Int 163: 107173, 2022.
47. Okada M, Matsuzawa A, Yoshimura A and Ichijo H: The lysosome rupture-activated TAK1-JNK pathway regulates NLRP3 inflammasome activation. J Biol Chem 289: 32926-32936, 2014.
48. Dickinson RJ and Keyse SM: Diverse physiological functions for dual-specificity MAP kinase phosphatases. J Cell Sci 119 (Pt 22): 4607-4615, 2006.
49. Ajizian SJ, English BK and Meals EA: Specific inhibitors of p38 and extracellular signal-regulated kinase mitogen-activated protein kinase pathways block inducible nitric oxide synthase and tumor necrosis factor accumulation in murine macrophages stimulated with lipopolysaccharide and interferon-gamma. J Infect Dis 179: 939-944, 1999.
50. An Y, Zhang H, Wang C, Jiao F, Xu H, Wang X, Luan W, Ma F, Ni L, Tang X, *et al*: Activation of ROS/MAPKs/NF-kB/NLRP3 and inhibition of efferocytosis in osteoclast-mediated diabetic osteoporosis. FASEB J 33: 12515-12527, 2019.
51. Dong Z, Zhuang Q, Ye X, Ning M, Wu S, Lu L and Wan X: Adiponectin Inhibits NLRP3 inflammasome activation in nonalcoholic steatohepatitis via AMPK-JNK/ErK1/2-NFκB/ROS signaling pathways. Front Med (Lausanne) 7: 546445, 2020.
52. Welsbie DS, Ziogas NK, Xu L, Kim BJ, Ge Y, Patel AK, Ryu J, Lehar M, Alexandris AS, Stewart N, *et al*: Targeted disruption of dual leucine zipper kinase and leucine zipper kinase promotes neuronal survival in a model of diffuse traumatic brain injury. Mol Neurodegener 14: 44, 2019.
53. Lin C, Wu F, Zheng T, Wang X, Chen Y and Wu X: Kaempferol attenuates retinal ganglion cell death by suppressing NLRP1/NLRP3 inflammasomes and caspase-8 via JNK and NF-κB pathways in acute glaucoma. Eye (Lond) 33: 777-784, 2019.
54. Chu X, Wang C, Wu Z, Fan L, Tao C, Lin J, Chen S, Lin Y and Ge Y: JNK/c-Jun-driven NLRP3 inflammasome activation in microglia contributed to retinal ganglion cells degeneration induced by indirect traumatic optic neuropathy. Exp Eye Res 202: 108335, 2021.
55. Liu R, Liu R, Liu C, Gao A, Wang L, Tang H, Wu Q, Wang X, Tian D, Qi Z and Shen Y: NEK7-Mediated Activation of NLRP3 inflammasome is coordinated by potassium Efflux/Syk/JNK signaling during staphylococcus aureus infection. Front Immunol 12: 747370, 2021.
56. Li J, Cao F, Yin HL, Huang ZJ, Lin ZT, Mao N, Sun B and Wang G: Ferroptosis: Past, present and future. Cell Death Dis 11: 88, 2020.
57. Cao JY, Poddar A, Magtanong L, Lumb JH, Mileur TR, Reid MA, Dovey CM, Wang J, Locasale JW, Stone E, *et al*: A genome-wide haploid genetic screen identifies regulators of glutathione abundance and ferroptosis sensitivity. Cell Rep 26: 1544-1556 e8, 2019.
58. Forcina GC and Dixon SJ: GPX4 at the crossroads of lipid homeostasis and ferroptosis. Proteomics 19: e1800311, 2019.
59. Yan N and Zhang JJ: The emerging roles of ferroptosis in vascular cognitive impairment. Front Neurosci 13: 811, 2019.

60. Kagan VE, Mao G, Qu F, Angeli JP, Doll S, Croix CS, Dar HH, Liu B, Tyurin VA, Ritov VB, *et al*: Oxidized arachidonic and adrenic PEs navigate cells to ferroptosis. Nat Chem Biol 13: 81-90, 2017.
61. Li DD, Wang LL, Deng R, Tang J, Shen Y, Guo JF, Wang Y, Xia LP, Feng GK, Liu QQ, *et al*: The pivotal role of c-Jun NH2-terminal kinase-mediated Beclin 1 expression during anticancer agents-induced autophagy in cancer cells. Oncogene 28: 886-898, 2009.
62. Otterbein LE, Bach FH, Alam J, Soares M, Tao Lu H, Wysk M, Davis RJ, Flavell RA and Choi AM: Carbon monoxide has anti-inflammatory effects involving the mitogen-activated protein kinase pathway. Nat Med 6: 422-428, 2000.
63. Yang J, Mo J, Dai J, Ye C, Cen W, Zheng X, Jiang L and Ye L: Cetuximab promotes RSL3-induced ferroptosis by suppressing the Nrf2/HO-1 signalling pathway in KRAS mutant colorectal cancer. Cell Death Dis 12: 1079, 2021.